

Gold Nanoparticles and [PEDOT-Poly(*D,L*-Lactic Acid)] Composite: Synthesis, Characterization and Application to H₂O₂ Sensing

Aruã C. da Silva,^a Marco A. O. S. Minadeo^a and Susana I. C. de Torresi^{✉*,a}

^aInstituto de Química, Universidade de São Paulo, Av. Professor Lineu Prestes, 748, 05508-000 São Paulo-SP, Brazil

Biocompatible electrochemical devices are challenging to develop due to the toxicity of many advanced electrode materials and the difficulty to degrade the discarded material. Few recent advances were made in the synthesis of conducting biodegradable composites of polymers for electrode materials. In this article we describe the synthesis of two new inorganic/organic nanocomposites of Au nanoparticles and conducting polymers based on the biodegradable polymer poly(*D,L*-lactic acid) (PDLLA): Au nanoparticles/oligomers of 3,4-ethylenedioxythiophene (EDOT)-PDLLA and Au nanoparticles with poly(3,4-ethylenedioxythiophene) (PEDOT)-PDLLA. The nanocomposites were carefully analyzed; the gold nanoparticles mean sizes were 8 ± 3 and 7 ± 2 nm, respectively. ¹H and ¹³C nuclear magnetic resonance (NMR) demonstrated the polymerization of EDOT-PDLLA made through one-pot reaction with Au^{III} precursor. Raman spectra show that PEDOT-PDLLA is formed in the synthesis of Au/PEDOT-PDLLA. The immobilization of Au/PEDOT-PDLLA on glassy carbon electrodes is easy and more stable than the immobilization of simple PEDOT. Au/PEDOT-PDLLA catalyzes the reduction of H₂O_{2(aq)}, which was detected by chronoamperometry. The sensor is stable and presents sensitivity of 8.36×10^{-3} A mol⁻¹ L cm⁻², linear range of 1-45 mmol L⁻¹ and limit of detection of 0.17 mmol L⁻¹.

Keywords: electroactive biodegradable macromonomer, gold, PEDOT, nanocomposite

Introduction

Nanomaterials have wide-range implications to a variety of areas, including chemistry, physics, electronics, optics, materials science, and the biomedical sciences.¹ Applications include their use in electronic, optical, and mechanical devices,²⁻⁵ drug delivery,^{6,7} and bioencapsulation.⁸ Poly(3,4-ethylenedioxythiophene), or PEDOT, is an organic electronic-conducting polymer (these polymers are hereafter called conducting polymers), which is widely used in electrochemical devices, solar cells and molecular electronic devices, being currently the most used conducting polymer worldwide.^{9,10}

Among the noble metals used as nanoparticles to form composites of interest with conducting polymers, the most used is gold. The exceptional electric conductivity of gold and its stability are some of the reasons.¹¹ Metal nanoparticles in general are much less stable than the corresponding bulk phases. Atomic scale layers of metallic oxides are formed in the surface of Ag, Cu and Pd nanoparticles depending on

the reaction media. Nanocomposites of gold nanoparticles with PEDOT have been deeply studied as electrochromic layer for electrochromic devices.¹²⁻²⁵

A relatively new class of materials are the biodegradable conducting polymers with biocompatible properties suitable for biomedical applications in living cells, bacteria and live organisms.²⁶ Several polymers combinations and inorganic/organic composites have been synthesized and described for this purpose. Boutry *et al.*²⁷ prepared the composites of poly(*D,L*-lactic acid) (PDLLA) with polypyrrole (PPy), and poly(caprolactones) (PCL) with PPy, and investigated their properties. PDLLA and PCL are both polyesters, polymers easily degradable by microorganisms or hydrolysis, which attack the ester bonds. Polyesters are also usually biocompatible because their monomer contents are based on organic acids common in living body. This strategy allowed obtaining a synergic, high-conducting material. Kuang *et al.*²⁸ developed a composite of carbon nanotubes and PDLLA. Yet, Xu *et al.*²⁹ synthesized polyurethanes with 1S-(+)-10-camphorsulfonic acid. The polyurethanes presented great elasticity and feasible conductivity when

*e-mail: storresi@iq.usp.br

hydrated. Moradpour *et al.*³⁰ prepared a material of palladium nanoparticles/ethylenediamine-functionalized cellulose/carbon-based paste, which showed catalytic activity for the hydrogen production. Mondal and Sharma³¹ described the preparation of a nanoblend of poly(butylene-adipate-*co*-terephthalate) with PPy by electrospinning. The blend is hydrophilic, biocompatible and conducting. All presented works used more than one polymer or component, being one of them a π -conjugated polymer on the final material or composite.

For biomedical applications, conducting polymers usually present some advantages towards metals and semiconductors in terms of biocompatibility, but modification strategies are usually required to improve them when thinking in a device.³² Recently, it was reported by our group the synthesis of a new electroactive macromonomer of 3,4-ethylenedioxythiophene (EDOT)-PDLLA,³³ which can play an important role in the synthesis of different conducting and biodegradable materials based on PEDOT and PDLLA chemistry. The polymerization of this electroactive macromonomer was tried by electrochemical methods, but (i) only oligomers were formed due to the high solubility in organic solvents, and (ii) no electroactive properties were found. Additionally, the chemical synthesis of a new PEDOT-*co*-PDLLA copolymer³⁴ with conductivity, biodegradability and noncytotoxicity properties tested for embryonic stem cells (E14.tg2a) was reported by using the electroactive macromonomer.

The challenges on the development of biomaterials with electroactivity for biosensing or to be applied in a biointerface are (i) the lack of biocompatibility of inorganic/organic composites; (ii) to immobilize films simply and efficiently on the substrates and (iii) the electrochemical stability. In this context, the gold nanoparticles are emerging as a promising candidate in nanomedicine due to its own biocompatible properties.³⁵⁻³⁷ In addition, the PDLLA has generally appeared to display a superior biocompatibility, being suitable for biomaterial devices.^{38,39}

In the present study, it was reported the synthesis of two novel conducting biodegradable polymer-based nanocomposites loaded with gold nanoparticles: Au/o-EDOT-PDLLA and Au/PEDOT-PDLLA nanocomposites. The Au/o-EDOT-PDLLA nanocomposite presents gold nanoparticles in a matrix of EDOT-PDLLA oligomers, but does not presented enough π -conjugation for electroactive properties, while the Au/PEDOT-PDLLA nanocomposite was further oxidized (increasing the π -conjugated chain and achieving conductivity) and it was investigated as an electrochemical sensor for hydrogen peroxide analysis.

Experimental

Chemicals

(2,3-Dihydrothieno[3,4-*b*][1,4]dioxin-2-yl)methanol (EDOT-CH₂-OH), 3,6-dimethyl-1,4-dioxane-2,5-dione (*D,L*-lactide), 3,4-ethylenedioxythiophene (EDOT, 97%), poly(sodium 4-styrenesulfonate) (NaPSS), organometallic catalyst tin(II)-2-ethylhexanoate (Sn(oct)₂, 92.5-100.0%), gold(III) chloride hydrate (HAuCl₄.xH₂O, 99.9%), ammonium persulfate (98%) and hydrogen peroxide solution (30% m/m in water) were obtained from Sigma-Aldrich. Toluene (99.5%), acetonitrile (99.5%) and dimethyl sulfoxide (DMSO, 99.5%) were purchased from Synth and were distilled before use. All aqueous solutions were prepared with deionized water (18.2 M Ω cm).

Synthesis of the Au/PEDOT-PDLLA nanocomposites

The first step of the synthesis was to obtain an electroactive macromonomer of EDOT-PDLLA, which was developed in our previous study³⁴ (Figure 1a). Briefly, 3,6-dimethyl-1,4-dioxane-2,5-dione (2.76 g, 20 mmol), hydroxymethyl EDOT (100 mg, 0.6 mmol) and tin(II)-2-ethylhexanoate (0.016 mL, 0.05 mmol) were stirred at 110 °C with 7 mL of toluene for 24 h. The solvent was removed by distillation under reduced pressure (2000 Pa, 60 °C). The obtained solid product was purified by recrystallization with a 1:4 hexane/methanol mixture, separated by decantation and vacuum dried until constant mass. The yield obtained from this procedure was 98%. ¹H nuclear magnetic resonance (NMR) (500 MHz, CDCl₃) δ 1.48-1.83 (m, 3H, H^b), 3.80-3.90 (m, 2H, H^e), 4.07-4.13 (m, 1H, H^d), 4.21-4.28 (m, 2H, H^c), 5.00-5.30 (m, 1H, H^g), 6.35 (s, 2H, H^a); ¹³C NMR (500 MHz, CDCl₃) δ 16.7 (C^h), 66.7 (C^c), 69.0 (C^g), 69.2 (C^e), 72.5 (C^d), 116.4 (C^a), 129.0 (C^b), 169.4 (C^f).

Gel permeation chromatography (GPC) indicated a number average molecular weight (M_n) of 3779 Da, molecular weight (M_w) of 5517 Da and a polydispersity index of 1.46.

The second step was to obtain Au/o-EDOT-PDLLA nanocomposite by modifying the previously reported route⁴⁰ (Figure 1b). Briefly, 10 μ L of EDOT-PDLLA was added to 10 mL of acetonitrile solution containing 0.01% m/v NaPSS. The solution was stirred and 250 μ L of HAuCl₄ aqueous solution (1 mmol L⁻¹) was added slowly, maintaining the stirring for 24 h. After the period, the dispersion turns into light purple color, thus the Au/o-EDOT-PDLLA nanocomposite was followed by UV-Vis spectroscopy (HP8453 diode array spectrophotometer, Hewlett Packard) (Figure 2a).

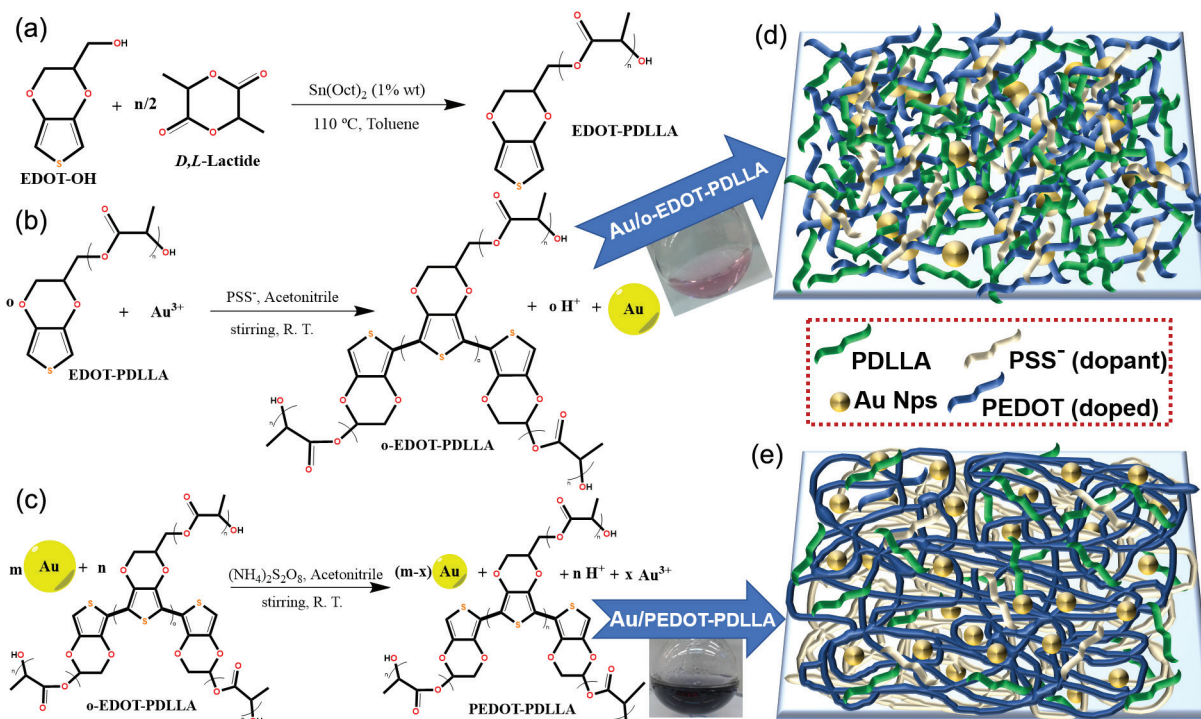


Figure 1. Synthesis reaction to obtain (a) the electroactive macromonomer of EDOT-PDLLA; (b) the nanocomposites of Au/o-EDOT-PDLLA and (c) Au/PEDOT-PDLLA. Schematic representation of the (d) Au/o-EDOT-PDLLA film and (e) Au/PEDOT-PDLLA film.

The third step aimed at obtaining Au/PEDOT-PDLLA nanocomposite (Figure 1c) based on the oxidation of EDOT-PDLLA oligomers by a stronger oxidant agent ($K_2S_2O_8$). It was added 125 mg of potassium persulfate (excess) to the same pot of the second step and kept stirring under room temperature for 24 h. The ammonium persulfate is insoluble in acetonitrile, thus after the period the ammonium persulfate decanted and only the soluble part was used containing the Au/PEDOT-PDLLA nanocomposite.

Characterization of the Au/PEDOT-PDLLA nanocomposites

UV-Vis-NIR (near infrared) spectrophotometry was performed with an HP8453 spectrophotometer

from Hewlett Packard and quartz and/or plastic optical cuvettes.

1H NMR spectra were recorded on a Bruker AIII 500 MHz spectrometer. Chloroform-*d* ($CDCl_3$) was used as solvent and tetramethylsilane (TMS) served as the internal standard.

Raman microscopies were performed with a Renishaw inVia Raman microscope with a Renishaw red laser of 636 nm wavelength.

Transmission electron microscopy (TEM) was performed with a JEOL JEM-2100 microscope (end point detection (EPD) of acceleration = 200 kV, LaB₆ filament) coupled with a silicon drift-type X-MaxN 80T energy dispersion spectra (EDS) from Oxford Instruments, controlled

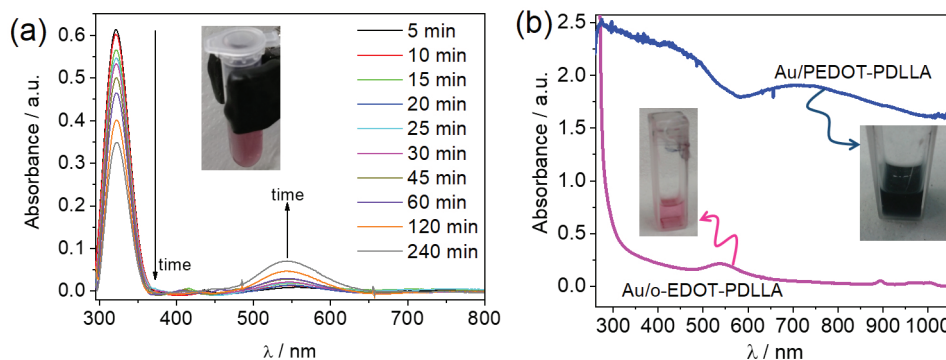


Figure 2. UV-visible spectra of (a) reaction of $HAuCl_4$ with EDOT-PDLLA with time and (b) comparison between the final spectra of Au/o-EDOT-PDLLA and Au/PEDOT-PDLLA.

by software AZtec INCA, and with a JEOL JEM-3010 (EPD of acceleration = 300 kV) and copper/carbon films TEM grids (diameter (d) = 3 mm, 400 mesh, from Ted Pella) were used. For the size particle analysis, it was used more than ten different images at different scales (20, 10 and 5 nm) for each nanocomposite and it was processed by using ImageJ⁴¹ and OriginLab 2018 software.⁴²

Electrochemical methods

The electrochemical experiments were performed with the bipotentiostat PGSTAT 302N and with the multi-potentiostat M101 from Metrohm Autolab, controlled by software NOVA 2.1 from Metrohm Autolab.

Glassy carbon electrodes (GCE) with $d = 3$ mm (area = 7.07 mm², from BASi) with polytetrafluoroethylene (PTFE) bodies were used as working electrodes. Prior to use the GCE were polished in a polishing machine, with suspensions of 1000, 500 and 300 nm size alumina nanoparticles. The electrodes were immersed in HCl_(conc):H₂O 1:1 (v/v), washed with water, immersed in HNO₃:H₂O 1:1 (v/v), washed with water and, when necessary, electrochemically cycled in 1 mol L⁻¹ H₂SO_{4(aq)} between -1.2 and +0.4 V (*versus* Ag/AgCl/KCl_(sat)) at 0.05 V s⁻¹ for 20 cycles. A platinum plate (from Impalla Metals) and a Ag/AgCl/KCl_(3 mol L⁻¹) electrode (from BASi) were used as counter and reference electrodes, respectively.

The immobilization of Au/PEDOT-PDLLA nanocomposite over GCE was performed by casting. First, 1 mL of the reaction suspensions were centrifuged in Eppendorf flasks in an appropriate centrifuge at 13400 rpm for 30 min, in order to precipitate the nanoparticles. The supernatants were discarded, 1 mL DMSO was added and the suspensions were sonicated in an ultrasound bath for the time necessary to resuspend the Au/PEDOT-PDLLA nanocomposite in DMSO that finally was drop casted onto GCE electrode surface.

For the electrochemical experiments with GCE, N_{2(g)} was bubbled in the electrolytes for at least 15 min to deoxygenate the solution and N_{2(g)} atmosphere was kept above it during the experiments.

Results and Discussion

Synthesis of the Au/PEDOT-PDLLA nanocomposites

The one-pot synthesis of two different proposed nanocomposites of Au/o-EDOT-PDLLA and Au/PEDOT-PDLLA is presented in Figure 1.

The first step of the one-pot synthesis of a modified electroactive macromonomer based on EDOT-PDLLA was

developed by our group³³ (Figure 1a). Herein, we decided to use the organometallic catalyst for the synthesis in order to obtain a higher molecular weight of the PDLLA chain, aiming better final properties in terms of processability (ease in obtaining films by spin coating and solubility in organic solvents). In our previous study,³³ it was found that EDOT-PDLLA can be electropolymerized, but only a few oligomers can be obtained, with no adhesion to the electrode surface, probably due to the increased solubility in organic solvent of the PDLLA part.

The second step of synthesis of the nanocomposite of Au/o-EDOT-PDLLA was obtained based on a modification of route proposed previously by Augusto *et al.*,⁴⁰ as shown in Figure 1b. When the Au³⁺ salt (HAuCl₄) is added to the reaction media, it starts the reduction of Au³⁺ to Au⁰ (nanoparticles) due to the presence of the EDOT-PDLLA, which is oxidized to form the EDOT⁺-PDLLA radical acting as an initiator to propagate the polymerization reaction to obtain oligomers of EDOT-PDLLA, represented as o-EDOT-PDLLA, with reaction media changing from colorless to light purple. The Au/o-EDOT-PDLLA composite does not present electroactivity due to (i) low conjugation length on the oligomers formed of EDOT and (ii) the higher amount of the PDLLA shielding the oligomers, avoiding electrical contact with Au nanoparticles and the electrode. Figure 1d corresponds to the representation of the Au/o-EDOT-PDLLA nanocomposite film with a matrix of o-EDOT-PDLLA/PSS loaded with Au nanoparticles.

The third step of synthesis is the obtaining of Au/PEDOT-PDLLA nanocomposite, presented in Figure 1c. In this case, it was used persulfate (S₂O₈²⁻, E⁰ = +2.010 V *versus* standard hydrogen electrode (SHE))⁴³ as oxidant agent, which is stronger than AuCl₄⁻ (E⁰ = +1.002 V *versus* SHE),⁴³ to effectively form PEDOT by further oxidation of the EDOT oligomers and enhance the electrical properties of the nanocomposite. Afterwards the reaction media turns into a dark blue color, very characteristic of PEDOT. It is important to mention that a tiny amount of Au nanoparticles is also oxidized to Au³⁺ again, resulting in smaller nanoparticle size after the reaction, supported by TEM images and histogram of particle size analysis on Figure 3. Figure 1e corresponds to the representation of the Au/PEDOT-PDLLA nanocomposite film with a matrix of PEDOT-PDLLA/PSS loaded with smaller Au nanoparticles.

Spectroscopic characterization of Au/PEDOT-PDLLA nanocomposites

The UV-visible spectroscopy was used to follow the second and third steps of the experimental procedure, as presented in Figure 2.

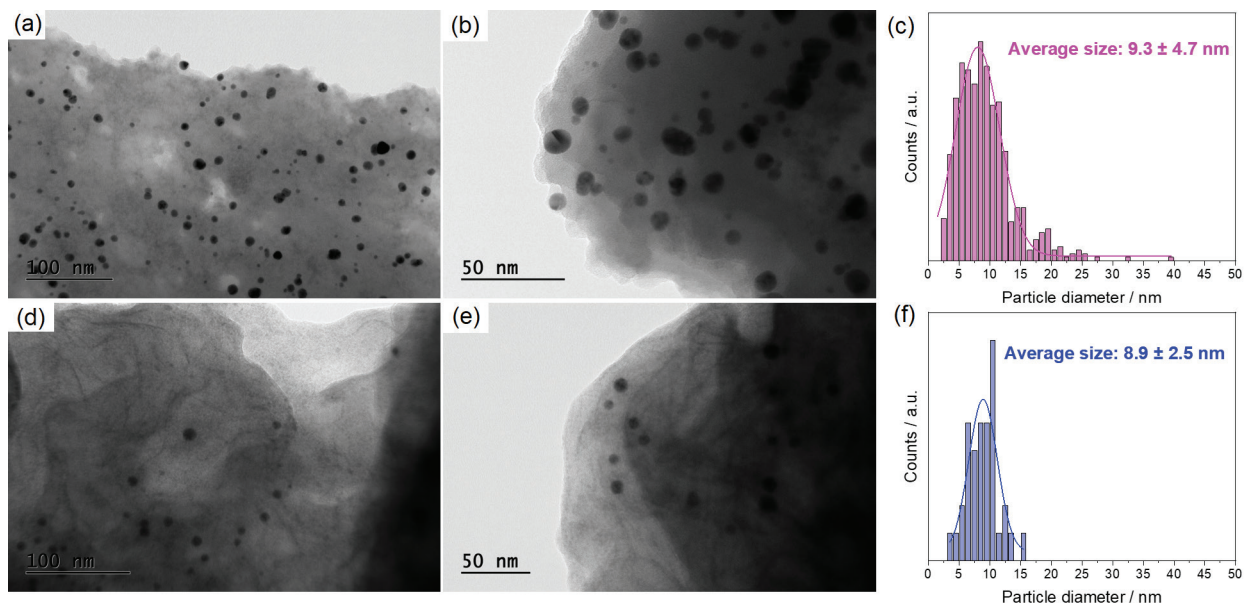


Figure 3. Transmission electron microscopy images of (a, b) Au/o-EDOT-PDLLA and (d, e) Au/PEDOT-PDLLA at 100 and 50 nm scale, respectively. Histogram of particle size analysis for (c) Au/o-EDOT-PDLLA and (f) Au/PEDOT-PDLLA.

Figure 2a shows the UV-visible spectra for the second step reaction for the formations of Au/o-EDOT-PDLLA. It was possible to see a decrease in the band at 321 nm (related to consumption of the reagent Au^{3+}) with an increase in the band at 544 nm (attributed to surface plasmon resonance of the Au nanoparticles).⁴⁴ Figure 2b presents the final spectra of UV-visible absorption for the nanocomposites Au/o-EDOT-PDLLA and Au/PEDOT-PDLLA. It was possible to observe that for Au/PEDOT-PDLLA nanocomposite (dark blue color) it presents absorption throughout the entire spectrum due to the obtaining of conjugated chains of PEDOT, and the surface plasmon resonance band characteristic for the Au

nanoparticles is not clearly observed when compared to the Au/o-EDOT-PDLLA nanocomposite spectrum.

The ^1H NMR and Raman spectroscopies were used to characterize the nanocomposite formation, as presented in Figure 4.

Figure 4a shows ^1H NMR spectrum of the electroactive macromonomer of EDOT-PDLLA (in black), the pure PEDOT-co-PDLLA (in blue) and Au/o-EDOT-PDLLA (in pink). The multiplets at 5.15 and 1.50 ppm are attributed to the CH and CH_3 of the PDLLA chain, respectively. The singlet in 6.36 ppm corresponds to hydrogen electropolymerizable on thiophene group (vicinal to sulfur) and it is well defined for EDOT-PDLLA,³³ while

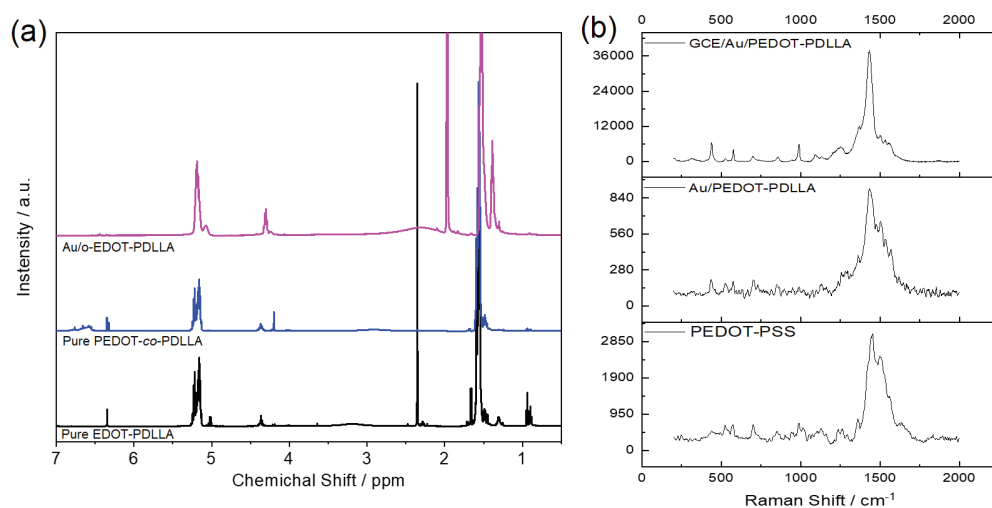


Figure 4. (a) ^1H NMR spectra for pure EDOT-PDLLA (black); pure PEDOT-co-PDLLA (blue) and the nanocomposite of Au/o-EDOT-PDLLA (pink); (b) Raman spectra of Au/PEDOT-PDLLA nanocomposite film covering glassy carbon electrode (top); aqueous dispersion of Au/PEDOT-PDLLA nanocomposite (middle) and aqueous solution of PEDOT-PSS (bottom).

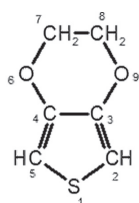
Table 1. Raman spectra bands assignments for composite materials

Sample	Raman band shift / cm ⁻¹										
	1	2	3	4	5	6	7	8	9	10	11
GCE/Au/ PEDOT-PDLLA	1432	1504	700	990	–	1535	1368	1253	1129	–	440
Au/PEDOT-PDLLA _(s)	1431	1501	703	–	–	1536	1363	1268	1131	1096	435
PEDOT/ PSS _(aq)	1453	1499	700	989	–	–	1362	1259	1128	–	–

Bands: 1: symmetric stretching C2=C3 for PEDOT doped; 2: asymmetrical stretching C2=C3; 3: symmetrical bending C5—S1—C2; 4: oxyethylene ring bending; 5 and 6: asymmetric stretching C2=C3; 7: C2=C3 stretching; 8: interring stretching; 9 and 10: C—O—C bending; 11: from contaminant.^{45,46} GCE: glassy carbon electrode; PEDOT-PDLLA: poly(3,4-ethylenedioxythiophene)-poly(*D,L*-lactic acid); PSS: poly(styrenesulfonate).

for PEDOT-*co*-PDLLA spectrum (blue) it is weaker and there are some shift to higher chemical shifts as a multiplet due to the different PEDOT chain lengths. For the Au/*o*-EDOT-PDLLA spectrum the same signal is very weak and looks like a multiplet, suggesting the oligomerization of EDOT-PDLLA. Additionally, at the region of 3.95-4.45 ppm it was possible to see a well-defined singlet at 4.20 ppm for the PEDOT-*co*-PDLLA spectrum, which corresponds to the hydrogens close to ethylenedioxy group on PEDOT chains which is not present on EDOT-PDLLA (black) because the modified EDOT-CH₂-OH have substituents on ethylenedioxy group leading for three multiplet-like signals in the same region,³³ but the Au/*o*-EDOT-PDLLA nanocomposite (pink) presents a multiplet stronger and shifted to a lower chemical shift values, reinforcing the idea of oligomerization of EDOT-PDLLA.

Figure 4b presents Raman spectra of Au/PEDOT-PDLLA nanocomposite film covering GCE (top), pure Au/PEDOT-PDLLA nanocomposite (middle) and PEDOT-PSS (bottom). Table 1 presents the assigned bands of spectra in Figure 4b. The PEDOT presents the main band in 1426-1453 cm⁻¹ corresponding to the symmetrical stretching of C2=C3 and C4=C5 bonds of thiophene groups (sulfur is always C1, as shown in Figure 5)⁴⁵ and it is characteristic of oxidized bipolaron of PEDOT structure which is present for all spectra, excepting the Au/*o*-EDOT-PDLLA spectrum. PEDOT in the neutral state shows Raman resonant effect with 525 nm laser, while oxidized PEDOT presents Raman resonant effect with 1064 nm laser.⁴⁷⁻⁵¹ The spectra demonstrate that PEDOTs are present in the samples and that PEDOT-PDLLA is electronically

**Figure 5.** Atom labels for all EDOT-derived compounds in this article.

similar to PEDOT, even when the film is formed onto a GCE.

Transmission electron microscopy analysis of the Au/PEDOT-PDLLA nanocomposites

The Au/*o*-EDOT-PDLLA and Au/PEDOT-PDLLA nanocomposites were analyzed by transmission electron microscopy (TEM) as shown in Figure 3.

Figure 3 shows the Au nanoparticles appearing in black, while the polymer around is lighter (grey). It was possible to observe for the Au/*o*-EDOT-PDLLA (Figure 3c) a higher amount of Au nanoparticles within 9.3 ± 4.7 nm size, while for Au/PEDOT-PDLLA there is lower number of nanoparticles, although they are a bit smaller and presented lower dispersity, 8.9 ± 2.5 nm (Figure 3f). However, it was expected, from the route synthesis, once adding persulfate to oxidize the EDOT-PDLLA oligomers, the Au nanoparticles should be also partially oxidized, dissolving the Au nanoparticles.

A further investigation on TEM images were the acquisition of EDS spectra, as shown in Figure 6.

Figure 6 shows the energy dispersion X-ray fluorescence spectra in different spots, Au nanoparticle or polymeric matrix, for Au/*o*-EDOT-PDLLA and Au/PEDOT-PDLLA nanocomposites. Several images and spots were analyzed; hence not big differences were noticed between spectra for the same type of spot. The C and Cu signals on the energy dispersion spectra are related to the Cu/C grid and the O signals is not clearly identified from the sample, environment or template, so it was not analyzed. The energy dispersion spectra for Au/*o*-EDOT-PDLLA (Figure 6B) presents signals for Au nanoparticles at 1.65, 2.14, 9.73 and 11.45 keV. A more relevant signal for the polymeric spots was the S at 2.32 keV, which is related to the thiophene groups, being stronger for the Au/PEDOT-PDLLA (Figure 6D) than Au/*o*-EDOT-PDLLA, which evidences the PEDOT formation with more thiophene groups. Additionally, the Au signals are stronger on Au/*o*-EDOT-PDLLA spectra, indicating the oxidation of

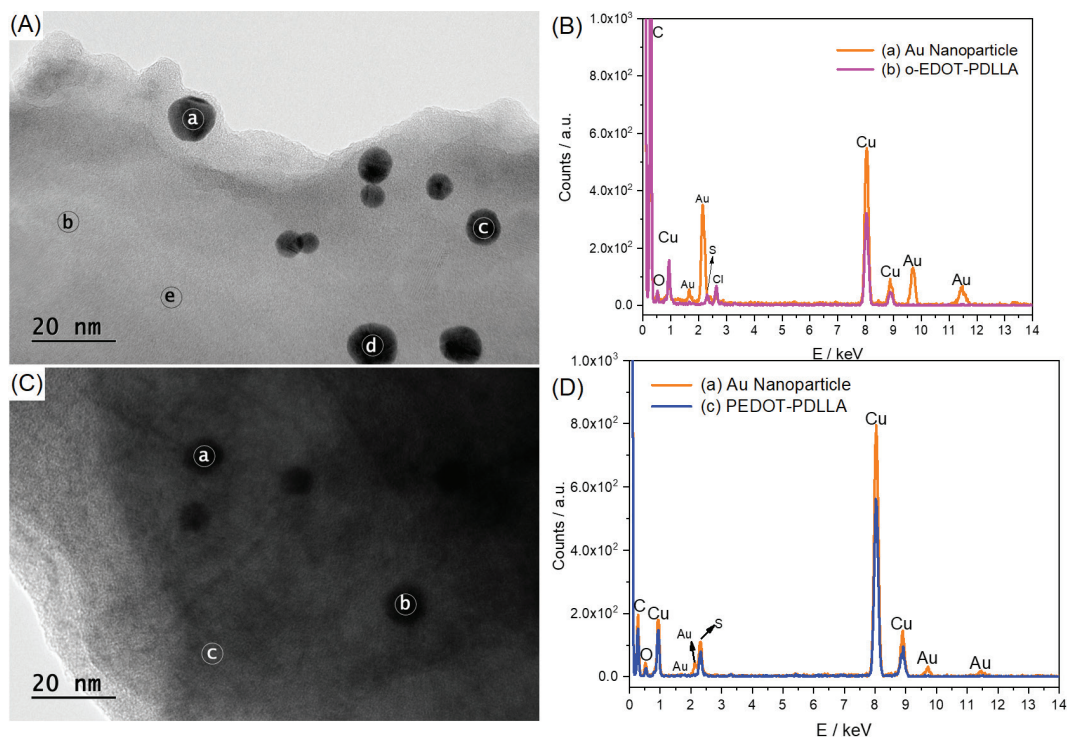


Figure 6. Transmission electron microscopy images of (A) Au/o-EDOT-PDLLA and (C) Au/PEDOT-PDLLA at 20 nm scale; (B, D) energy dispersion spectra for (a) Au nanoparticle regions; (b) o-EDOT-PDLLA and (c) PEDOT-PDLLA regions.

Au nanoparticles by persulfate in the third synthesis step.

One-layer film of the Au/PEDOT-PDLLA nanocomposite was deposited onto a GCE and the morphology of the nanocomposite was investigated by scanning electron microscopy (Figure S1, Supplementary Information section). It was possible to observe the film uniformly covering the GCE and presenting a globular structure with some brighter spots, apparently related to the Au nanoparticles and its aggregates.

Electrochemical characterization of the Au/PEDOT-PDLLA nanocomposites for H_2O_2 sensing

After spectroscopic and physical characterization, the Au/PEDOT-PDLLA nanocomposite was studied as an electrochemical sensor for the reduction of hydrogen peroxide. In alkaline medium, $\text{H}_2\text{O}_{2(\text{aq})}$ can be electrochemically reduced to $\text{OH}^-_{(\text{aq})}$ through the following reaction:



Applying a negative potential to the working electrode it is possible to promote the reaction in equation 1. For a better understanding of the electrochemical behavior of the Au/PEDOT-PDLLA nanocomposite, 5 layers (optimized number, Figure 7a) of the nanocomposite were deposited

over a GCE and cyclic voltammograms were performed increasing H_2O_2 concentration from 1-43 mmol L^{-1} , as shown in Figure 7b.

Figure 7 shows the j / E cyclic voltammograms of the Au/PEDOT-PDLLA nanocomposite. It is possible to observe the higher current response is obtained for 5 layers of the Au/PEDOT-PDLLA nanocomposite (Figure 7a). The 5 layers film Au/PEDOT-PDLLA nanocomposite deposited onto GCE in presence of increasing concentrations of H_2O_2 (Figure 7b) presented a good response to H_2O_2 reduction in a wide range of electric potential, thus it was selected -0.312 V versus $\text{Ag}/\text{AgCl}/\text{KCl}_{(\text{sat})}$ for analytical purposes in order to avoid side reactions.

Chronoamperometric experiments with different additions of H_2O_2 were performed for the film of Au/PEDOT-PDLLA nanocomposite deposited on glassy carbon, as observed in Figure 8.

Figure 8 shows a chronoamperometric curve recorded during the addition of hydrogen peroxide and the analytical curve of the Au/PEDOT-PDLLA nanocomposite. At the initial state, the current density stabilized for a few seconds near to zero. The first 10 additions of $\text{H}_2\text{O}_{2(\text{aq})}$ (until 6750 s) were nominal of 1 mmol L^{-1} , while the last additions were of 10 mmol L^{-1} . The increments of current density due to the additions of +1 mmol L^{-1} are fast and uniform, being $j \propto [\text{H}_2\text{O}_2]$ a linear curve. It increases (in module) and stabilizes in each step. For the higher amount

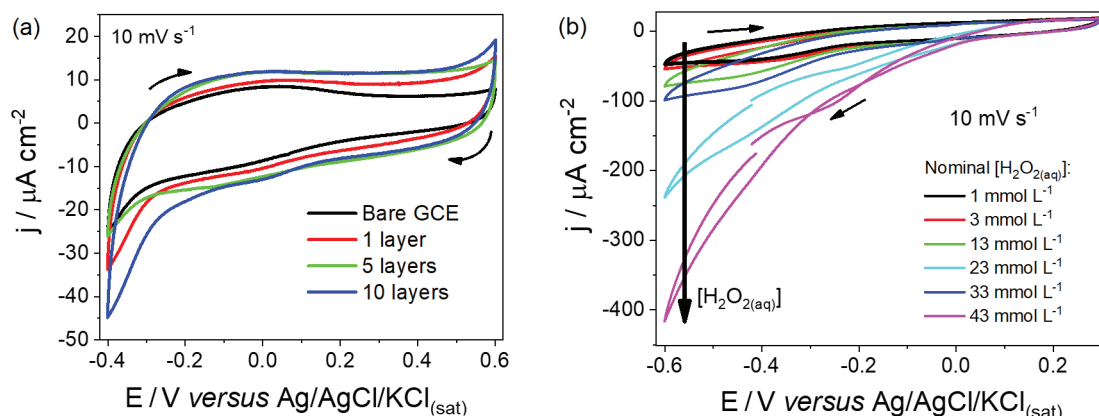


Figure 7. j / E cyclic voltammograms of (a) the 10th cycle of different Au/PEDOT-PDLLA film layers onto glassy carbon electrode voltammograms and (b) 5 layers film with increasing hydrogen peroxide concentrations: 1–43 mmol L⁻¹. Scan rate of 10 mV s⁻¹, in 20 mmol L⁻¹ phosphate buffer electrolytic solution (pH = 7.4).

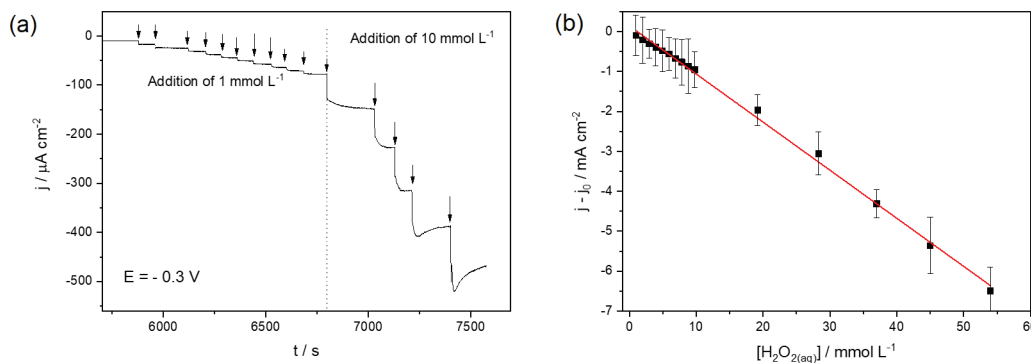


Figure 8. (a) Chronoamperogram for hydrogen peroxide detection with a film of Au/PEDOT-PDLLA deposited on glassy carbon electrode and (b) analytical curve for H₂O₂ detection, in 20 mmol L⁻¹ phosphate buffer electrolytic solution (pH = 7.4).

additions (+10 mmol L⁻¹) the current density increments are linear, but the response time is higher (Figure 8a). The analytical curve for the GCE/Au/PEDOT-PDLLA sensor was presented (Figure 8b) with linear range (LR) from 1 to 53 mmol L⁻¹, limit of detection (LOD) of 0.17 mmol L⁻¹ and sensitivity (S) of $8.36 \times 10^{-3} \text{ A mol}^{-1} \text{ L cm}^{-2}$.

Table 2 was used to compare the performance of GCE/Au/PEDOT-PDLLA to other PEDOT/nanoparticles-based amperometric sensors for H₂O_{2(aq)} described in the literature.

A usual way to decrease the energy necessary for H₂O₂ detection is immobilizing a mediator in the sensor, such as Prussian Blue (PB),⁵⁹ copper hexacyanoferrate,⁵⁵ hemoglobin (Hb),⁵⁷ among others. The sensor based on GCE/Au/PEDOT-PDLLA can be applied for H₂O₂ detection at -300 mV without adding any kind of mediator, at a potential used by similar sensors,⁶⁰ while there are some PEDOT-based sensors which can operate only at negative higher (in module) potentials (around -500 mV).^{52,53} The advantage of working in a more negative potential is that there are no redox reactions occurring simultaneously, such as oxidation of uric acid, ascorbic acid and dopamine

(usually present in real samples). This contributes to a better selectivity of the H₂O₂ sensor.

The advantage on using PDLLA on the Au/PEDOT-PDLLA nanocomposite is the biocompatibility and biodegradability; when thinking in sensors and biosensors for diagnosis analysis its properties are very desirable. In addition, it contributes for a better solubility in organic solvents becoming easy the processability of the nanocomposite. The presented approaches (Table 2) need more complicated methods for immobilization of the nanocomposites, such as using Nafion immobilization over the sensor,⁵⁴ physical adsorption (usually with bad adhesion to substrates)⁶⁰ or electrodeposition.^{53,55-59}

The sensors proposed by Lin *et al.*⁵³ (carbon nanotubes), Chen *et al.*⁵⁷ (nanowhiskers of PEDOT) and Nabid *et al.*⁶⁰ (nanofibers of PEDOT) present a great effect of surface area, influencing the detection limit and the sensitivity. Even though, the GCE/Au/PEDOT-PDLLA sensor presents a very high sensitivity ($8.36 \times 10^{-3} \text{ A mol}^{-1} \text{ L cm}^{-2}$) when compared to other sensors (Table 2), while the more sensitive needs to apply more energy for sensing (-550 mV).⁵²

Table 2. Parameters of electrochemical sensors of H₂O₂ containing PEDOT hybrids

Sensor	E / mV	LR / (mol L ⁻¹)	S / (A mol ⁻¹ L cm ⁻²)	LOD / (mol L ⁻¹)	Reference
SPC/PEDOT/NPpt ^a	-550	(1.62 × 10 ⁻⁶)-(6 × 10 ⁻³)	1.93 × 10 ⁻²	1.6 × 10 ⁻⁶	52
MWCNT/PEDOT ^b	-500	10 ⁻⁴ -(9.8 × 10 ⁻³)	–	(5 × 10 ⁻⁵)-10 ⁻²	53
Pd/PEDOT	-165	(2.84 × 10 ⁻⁶)-10 ⁻³	2.15 × 10 ⁻⁴	2.84 × 10 ⁻⁶	54
PEDOT/NPCu-Cu ₂ [Fe(CN) ₆] ^c	-200	10 ⁻⁶ -(5.4 × 10 ⁻⁴)	1.67 × 10 ⁻³	10 ⁻⁷	55
GCE/PEDOT/PSS/Pd ^d	–	10 ⁻⁴ -(5 × 10 ⁻³)	–	–	56
NW/PEDOT/NPAu/Hb ^e	-265	6 × 10 ⁻⁴ -(1.1 × 10 ⁻³)	3.13 × 10 ⁻⁴	6 × 10 ⁻⁴	57
GCE/PEDOT/NPAg	-40	–	–	6.1 × 10 ⁻⁷	58
PEDOT/NPPB ^f	-1	(5 × 10 ⁻⁷)-(8.39 × 10 ⁻⁶)	–	1.6 × 10 ⁻⁷	59
NFPEDOT/NPPd ^g	-312	(2 × 10 ⁻⁷)-(2.5 × 10 ⁻⁵)	–	5 × 10 ⁻⁸	60
GCE/Au/PEDOT-PDLLA	-312	(1.0 × 10 ⁻³)-(4.5 × 10 ⁻²)	8.36 × 10 ⁻³	1.7 × 10 ⁻⁴	present work

^aPoly(3,4-ethylenedioxythiophene) (PEDOT) and NPpt nanocomposite over screen-printed carbon (SPC) electrode; ^bmultiwall carbon nanotubes (MWCNT) and PEDOT nanocomposite over glassy carbon electrode (GCE); ^cnanocomposite of PEDOT and nanoparticles of Cu and copper hexacyanoferrate; ^drotating disc electrode; ^enanocomposite of PEDOT nanowhiskers (NW), NPAu and hemoglobin (Hb); ^fPrussian Blue (PB) and PEDOT nanocomposite; ^gPEDOT nanofibers and NPPd nanocomposite. E: electrical potential; LR: linear range; S: sensitivity; LOD: limit of detection; NP: nanoparticles; PSS: poly(styrenesulfonate); NF: nanofiber; PDLLA: poly(*D,L*-lactic acid).

Furthermore, the GCE/Au/PEDOT-PDLLA sensor presented a huge linear range reaching almost two decades (1.0 × 10⁻³ to 4.5 × 10⁻² mol), being suitable for relatively high concentrations. The wide detection range of the Au/PEDOT-PDLLA nanocomposite is probably related to the stable films formed through the PDLLA interaction with the small Au nanoparticles (< 10 nm) well connected to the PEDOT chains, enhancing its own electronic stability.

Conclusions

The synthesis of two novel conducting biodegradable polymer-based nanocomposites loaded with gold nanoparticles, Au/o-EDOT-PDLLA and Au/PEDOT-PDLLA nanocomposites, was presented.

The Au/o-EDOT-PDLLA nanocomposite presented the formation of Au nanoparticles with 8 ± 3 nm size followed by UV-visible spectroscopy and the oligomers of EDOT-PDLLA were confirmed by ¹H NMR spectra. No conductivity was observed for the o-EDOT-PDLLA, but it still can be useful for optical application (e.g., plasmonic effects).

The Au/PEDOT-PDLLA nanocomposite presented Au nanoparticles smaller than in the oligomers, with 7 ± 2 nm size, and the polymerization of PEDOT-PDLLA was confirmed by Raman spectroscopy. The nanocomposite formed films with organic solvents and its electrochemical behavior was optimized by cyclic voltammetry.

The film of Au/PEDOT-PDLLA nanocomposite was evaluated towards a hydrogen peroxide reduction reaction and is a promissory material for sensing because it presented a huge linear range (almost 2 decades) with sensitivity of 8.36 × 10⁻³ A mol⁻¹ L cm⁻², suitable for application at mmol L⁻¹ range.

Supplementary Information

Supplementary information is available free of charge at <http://jbcs.sbq.org.br> as PDF file and presents the photograph of electrode GCE/Au/PEDOT-PDLLA with the optimized 5 layers of the nanocomposite with SEM images of the film onto the electrode.

Acknowledgments

The authors gratefully acknowledge Brazilian agencies FAPESP (Process 2015/26308-7), CNPq and CAPES for their financial support. A. C. S. and M. A. O. S. M. thank FAPESP (Processes 2014/09353-6 and 2013/00322-8) for the scholarships.

References

- Bate, R. T.; *Sci. Am.* **1988**, 258, 96.
- Ahn, J.-H.; Kim, H.-S.; Lee, K. J.; Jeon, S.; Kang, S. J.; Sun, Y.; Nuzzo, R. G.; Rogers, J. A.; *Science* **2006**, 314, 1754.
- Maier, S. A.; Brongersma, M. L.; Kik, P. G.; Meltzer, S.; Requicha, A. A. G.; Atwater, H. A.; *Adv. Mater.* **2001**, 13, 1501.
- Ariga, K.; Mori, T.; Hill, J. P.; *Adv. Mater.* **2012**, 24, 158.
- Choi, S.; Lee, H.; Ghaffari, R.; Hyeon, T.; Kim, D.-H.; *Adv. Mater.* **2016**, 28, 4203.
- Hubbell, J. A.; Chilkoti, A.; *Science* **2012**, 337, 303.
- Kumar, C. S. S. R.; Mohammad, F.; *Adv. Drug Delivery Rev.* **2011**, 63, 789.
- Cheng, X.; Poenitzsch, V.; Cornell, L.; Tsao, C.; Potter, T.; *J. Encapsulation Adsorpt. Sci.* **2013**, 3, 16.
- Bulut, U.; Cirpan, A.; *Synth. Met.* **2005**, 148, 65.
- Woo, H. S.; Czerw, R.; Webster, S.; Carroll, D. L.; Park, J. W.; Lee, J. H.; *Synth. Met.* **2001**, 116, 369.

11. Welch, C. M.; Compton, R. G.; *Anal. Bioanal. Chem.* **2006**, *384*, 601.
12. Kondratiev, V. V.; Pogulaichenko, N. A.; Hui, S.; Tolstopjatova, E. G.; Malev, V. V.; *J. Solid State Electrochem.* **2012**, *16*, 1291.
13. Kondratiev, V. V.; Pogulaichenko, N. A.; Tolstopjatova, E. G.; Malev, V. V.; *J. Solid State Electrochem.* **2011**, *15*, 2383.
14. He, T.; Ma, Y.; Cao, Y.; Yin, Y.; Yang, W.; Yao, J.; *Appl. Surf. Sci.* **2001**, *180*, 336.
15. Prakash, S.; Rao, C. R. K.; Vijayan, M.; *Electrochim. Acta* **2009**, *54*, 5919.
16. Park, K. W.; *Electrochim. Acta* **2005**, *50*, 4690.
17. Cho, S. H.; Park, S.-M.; *J. Phys. Chem. B* **2006**, *110*, 25656.
18. Atta, N. F.; Galal, A.; El-Ads, E. H.; *Electrochim. Acta* **2012**, *69*, 102.
19. Liu, Y.-C.; Chuang, T. C.; *J. Phys. Chem. B* **2003**, *107*, 12383.
20. Giannetto, M.; Mori, G.; Terzi, F.; Zanardi, C.; Seeber, R.; *Electroanalysis* **2011**, *23*, 456.
21. Manesh, K. M.; Santhosh, P.; Gopalan, A.; Lee, K. P.; *Talanta* **2008**, *75*, 1307.
22. Selvaganesh, S. V.; Mathiyarasu, J.; Phani, K. L. N.; Yegnaraman, V.; *Nanoscale Res. Lett.* **2007**, *2*, 546.
23. Mumtaz, M.; Ouvrard, B.; Maillaud, L.; Labrugere, C.; Cloutet, E.; Cramail, H.; Delville, M. H.; *Eur. J. Inorg. Chem.* **2012**, 5360.
24. Lee, J. S.; Choi, Y.-J.; Wang, S.-J.; Park, H.-H.; Pyun, J. C.; *Phys. Status Solidi* **2011**, *208*, 81.
25. Selvan, B. S. T.; Spatz, J. P.; Klok, H.; Möller, M.; *Adv. Mater.* **1998**, 1996.
26. Mohanty, A. K.; Misra, M.; Hinrichsen, G.; *Macromol. Mater. Eng.* **2000**, 276-277, 1.
27. Boutry, C. M.; Müller, M.; Hierold, C.; *Mater. Sci. Eng., C* **2012**, *32*, 1610.
28. Kuang, T.; Chang, L.; Chen, F.; Sheng, Y.; Fu, D.; Peng, X.; *Carbon* **2016**, *105*, 305.
29. Xu, C.; Yepez, G.; Wei, Z.; Liu, F.; Bugarin, A.; Hong, Y.; *J. Biomed. Mater. Res.* **2016**, *104*, 2305.
30. Moradpour, A.; Ghaffarinejad, A.; Maleki, A.; Eskandarpour, V.; Motaharian, A.; *RSC Adv.* **2015**, *5*, 70668.
31. Mondal, K.; Sharma, A.; *RSC Adv.* **2016**, *6*, 94595.
32. Guimard, N. K.; Gomez, N.; Schmidt, C. E.; *Prog. Polym. Sci.* **2007**, *32*, 876.
33. da Silva, A. C.; Augusto, T.; Andrade, L. H.; de Torresi, S. I. C.; *Mater. Sci. Eng., C* **2018**, *83*, 35.
34. da Silva, A. C.; Semeano, A. T. S.; Dourado, A. H. B.; Ulrich, H.; de Torresi, S. I. C.; *ACS Omega* **2018**, *3*, 5593.
35. Shukla, R.; Bansal, V.; Chaudhary, M.; Basu, A.; Bhone, R. R.; Sastry, M.; *Langmuir* **2005**, *21*, 10644.
36. Nune, S. K.; Chanda, N.; Shukla, R.; Katti, K.; Kulkarni, R. R.; Thilakavathy, S.; Mekapothula, S.; Kannan, R.; Katti, K. V.; *J. Mater. Chem.* **2009**, *19*, 2912.
37. Ma, H.; Sun, J.; Zhang, Y.; Bian, C.; Xia, S.; Zhen, T.; *Biosens. Bioelectron.* **2016**, *80*, 222.
38. Williams, D. F.; *Biomaterials* **2008**, *29*, 2941.
39. Anderson, J. M.; Shive, M. S.; *Adv. Drug Delivery Rev.* **1997**, *28*, 5.
40. Augusto, T.; Teixeira Neto, É.; Teixeira Neto, Â. A.; Vichessi, R.; Vidotti, M.; de Torresi, S. I. C.; *Sol. Energy Mater. Sol. Cells* **2013**, *118*, 72.
41. Rueden, C. T.; Schindelin, J.; Hiner, M. C.; DeZonia, B. E.; Walter, A. E.; Arena, E. T.; Eliceiri, K. W.; *BMC Bioinformatics* **2017**, *18*, 529.
42. *Origin 2018*; OriginLab Corporation, Northampton, MA, USA, 2018.
43. Haynes, W. M.; *CRC Handbook of Chemistry and Physics*, 93rd ed.; CRC Press: Boca Raton, 2012.
44. Wang, Y.; Zeiri, O.; Neyman, A.; Stellacci, F.; Weinstock, I. A.; *ACS Nano* **2012**, *6*, 629.
45. Feng, X.; East, A. J.; Hammond, W. B.; Zhang, Y.; Jaffe, M.; *Polym. Adv. Technol.* **2011**, *22*, 139.
46. Slepicka, P.; Kasalkova, N. S.; Siegel, J.; Kolska, Z.; Bacakova, L.; Svorcik, V.; *Biotechnol. Adv.* **2015**, *33*, 1120.
47. Garreau, S.; Louarn, G.; Buisson, J. P.; Froyer, G.; Lefrant, S.; *Macromolecules* **1999**, *32*, 6807.
48. Garreau, A.; Duvail, J.-L.; *Adv. Opt. Mater.* **2014**, *2*, 1122.
49. Garreau, S.; Duvail, J. L.; Louarn, G.; *Synth. Met.* **2001**, *125*, 325.
50. Tran-Van, F.; Garreau, S.; Louarn, G.; Froyer, G.; Chevrot, C.; *Synth. Met.* **2001**, *119*, 381.
51. Duvail, J. L.; Rétho, P.; Garreau, S.; Louarn, G.; Godon, C.; Demoustier-Champagne, S.; *Synth. Met.* **2002**, *131*, 123.
52. Chang, L.-C.; Wu, H.-N.; Lin, C.-Y.; Lai, Y.-H.; Hu, C.-W.; Ho, K.-C.; *Nanoscale Res. Lett.* **2012**, *7*, 319.
53. Lin, K.; Tsai, T.; Chen, S.; *Biosens. Bioelectron.* **2010**, *26*, 608.
54. Jiang, F.; Yue, R.; Du, Y.; Xu, J.; Yang, P.; *Biosens. Bioelectron.* **2013**, *44*, 127.
55. Tsai, T.; Chen, T.; Chen, S.; *Int. J. Electrochem. Sci.* **2011**, *6*, 4628.
56. Smolin, A. M.; Novoselov, N. P.; Babkova, T. A.; Eliseeva, S. N.; Kondrat, V. V.; *Int. J. Electrochem. Sci.* **2015**, *70*, 846.
57. Chen, S. Y.; Gai, P.; Jin, L.; Zhu, D.; Tian, D.; Abdel-Halim, E. S.; Zhang, J.; Zhu, J.-J.; *J. Mater. Chem. B* **2013**, *1*, 3451.
58. Rad, A. S.; Ardjmand, M.; Jahanshahi, M.; Safekordi, A.-A.; *J. Nano Res.* **2012**, *16*, 77.
59. Wang, J.; Wang, Y.; Cui, M.; Xu, S.; Luo, X.; *Microchim. Acta* **2017**, 483.
60. Nabid, M. R.; Rezaei, S. J. T.; Hosseini, S. Z.; *Mater. Lett.* **2012**, *84*, 128.

Submitted: February 6, 2019

Published online: April 15, 2019

